HYDRODYNAMICS AND MIXING IN LAKES, RESERVOIRS, WETLANDS AND RIVERS

Contents

The Benthic Boundary Layer (in Rivers, Lakes, and Reservoirs)

A Lorke, University of Koblenz-Landau, Landau/Pfaly, Germany
S MacIntyre, University of California, Santa Barbara, CA, USA

Introduction

Definition and Relevance of the Benthic Boundary Layer

The benthic boundary layer (BBL) of lakes, reservoirs, and rivers constitutes that part of the water column that is directly influenced by the presence of the sediment–water interface. Similar to the surface mixed layer, it represents a hot spot not only of dissipation of kinetic energy, but also of biological activity and of geochemical transformation processes. These different processes are strongly coupled and interact with each other: While the hydrodynamic conditions are modified by biological activity, which changes the structure of the sediment surface, the release of dissolved solids from the sediment can modify the density stratification in the BBL. Moreover, the actual sediment surface cannot always be regarded as rigid since the BBL flow does not only modify the structure of the sediment surface, but it can also bring sediment particles into suspension, whereas at other sites or at other times, the particles resettle.

The BBL definition provided here and the more detailed discussions later explicitly refer to *direct* influences of the sediment surface. From a more general point of view, the BBL is of great importance for the entire water body, almost independent of the dimensions of the basin. Strong turbulence and mixing along the boundaries are known to be important for vertical mixing, and transport on a basin scale and biogeochemical processes at the sediment surface or within the sediment effect the distribution of relevant water constituents on scales much larger than the actual dimensions of the BBL. These larger-scale effects, however, require additional transport processes for energy and matter into or out of the BBL and are considered elsewhere.

A major characteristic of the BBL is the magnitude and the temporal dynamics of the physical forcing, i.e., the current velocity at the top of the BBL. Although in most rivers this forcing can be regarded as a steady-state unidirectional flow, its nature in deep and stratified lakes and reservoirs is more complex. In these, usually stratified, water bodies the major energy is provided by surface waves in the shallow littoral zone, by high-frequency internal waves at the depth of the thermocline and by basin-scale internal waves (seiches or Kelvin and Poincare waves) in the hypolimnion. Hence, the magnitude and temporal dynamics of the different forcing mechanisms range from current velocities of some 10 cm s^{-1} and time scales of seconds for surface waves, to typical current velocities of a few centimeters per second and

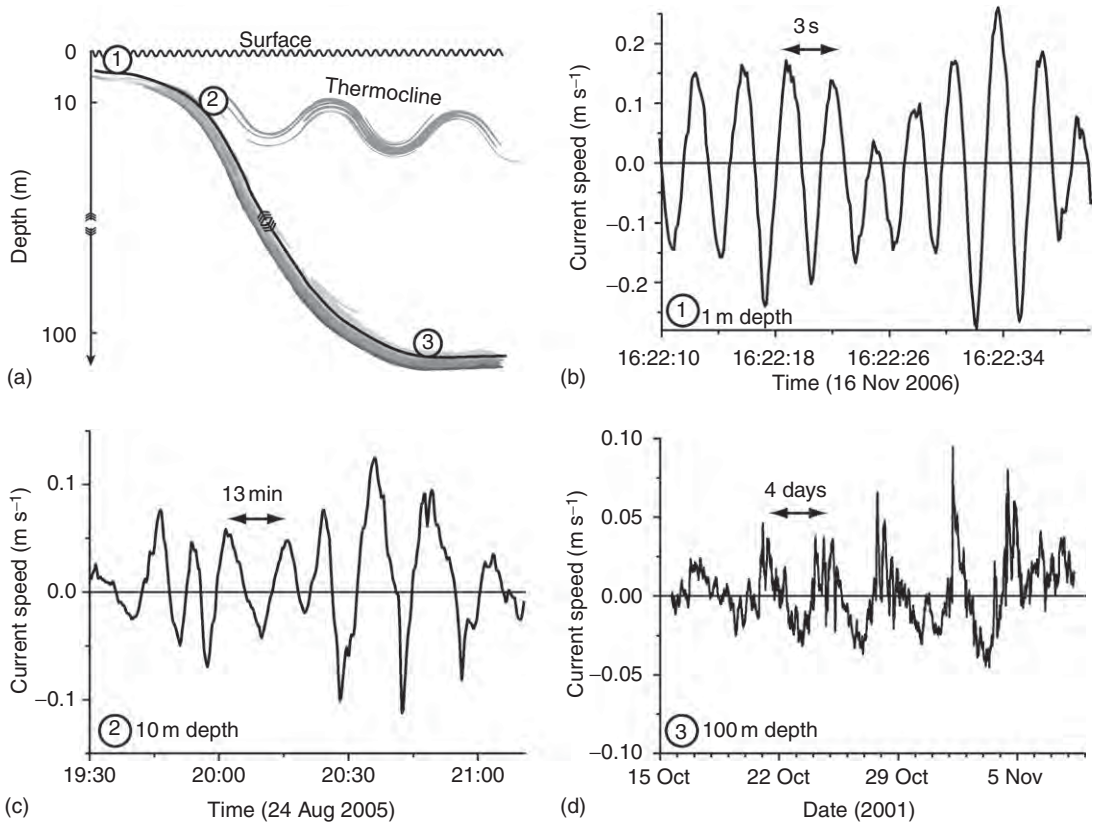

Figure 1 Typical near-bottom current velocities measured at various locations (depths) in a large Lake (Lake Constance) emphasizing the different periods and magnitudes of BBL forcing. (a) A schematic cross-section of the lake with the three sampling sites indicated by numbers. Near-bottom current velocities induced by surface waves at 1-m depth are shown in panel (b). Typical periods of surface waves in lakes are in the order of seconds. (c) Near-bottom current velocities measured at the depth of the seasonal thermocline (10-m depth). The observed current velocities are driven by propagating internal waves with periods between 8 and 20 min. Near-bottom currents at 100-m depth (d) are mainly driven by basin-scale internal waves. The major period of about four days is associated with a Kelvin wave. Note that several other basin-scale modes of oscillation (e.g., 12 h) are superimposed on this four-day period.

time scales of several hours to days for basin-scale internal waves (Figure 1).

Structure of the BBL

The BBL can be structured vertically according to the physical processes governing the vertical transport of momentum and solutes (Figure 2). In an outer layer (turbulent BBL) up to several meters above the sediment surface, this transport is governed by turbulent eddies and the associated mixing rates are high. While approaching the sediment surface down to scales where viscous forces suppress overturning turbulent motions, the vertical transport of momentum is governed by molecular viscosity and a viscous sublayer with a typical height of $O(1\,\text{cm})$ develops. The exchange of heat and dissolved solids and gases is eventually controlled by a diffusive sublayer with a height of $O(1\,\text{mm})$ directly at the sediment–water interface.

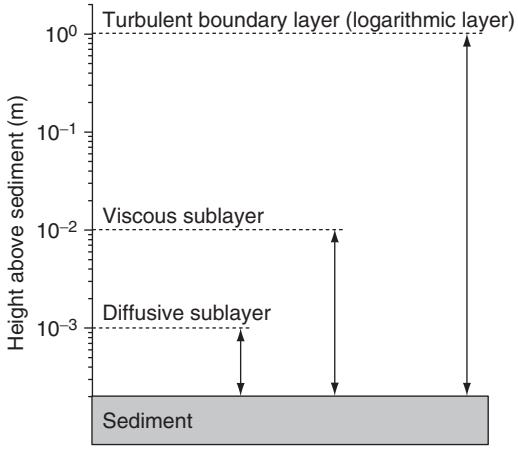

Figure 2 Idealized structure of the BBL on a flat sediment surface. Note that the heights provided by the logarithmically scaled axis represent order of magnitude estimates for typical conditions found in inland water bodies.

The Transport of Momentum

The Turbulent BBL

The equation for total average shear stress τ in a turbulent boundary layer is

$$\tau = \mu \frac{\mathrm{d}u}{\mathrm{d}z} + \rho \overline{u'w'} \quad [1]$$

where μ is dynamic viscosity, $\mathrm{d}u/\mathrm{d}z$ is the vertical velocity gradient, u' and w' are the fluctuating horizontal and vertical velocities, and the overbar denotes temporal averaging. While the first term on the right describes viscous shear, the second term is related to momentum transport by turbulent velocity fluctuations. In most aquatic systems, the Reynolds number associated with near-bottom flows is sufficiently high to sustain a turbulent boundary layer. Under such conditions, the first term on the right-hand side of eqn [1] may be negligible and turbulent shear stress is likely to dominate the shear stress computation.

On the basis of dimensional arguments, it can be assumed that the shear stress, τ, on the sediment surface is related to the current speed at a certain height above the sediment:

$$\tau = \rho C_{\mathrm{D}} U_{1\mathrm{m}}^2 \quad [2]$$

where ρ is the density, C_{D} an empirical constant ($\approx 1.5 \times 10^{-3}$), the so-called drag coefficient, and $U_{1\,\mathrm{m}}$ refers to the current speed measured at a height of 1 m above the sediment surface. Note that C_{D} depends on the reference height where the current speed was measured and a standard height of 1 m is assumed from now on. The bed shear stress τ is assumed to be constant throughout the boundary layer (constant stress layer) and it is used to define a turbulent velocity scale u_*, the so-called friction velocity:

$$u_* = \sqrt{\frac{\tau}{\rho}} \quad [3]$$

Dimensional analysis can then be used to deduce the velocity distribution $u(z)$ near the sediment surface, where z is the distance from the sediment surface. For a layer far enough from the boundary so that the direct effect of molecular viscosity on the flow can be neglected (the outer layer), the analysis results in

$$u(z) = \frac{u_*}{\kappa} \ln \frac{z}{z_0} \quad [4]$$

where $\kappa \approx 0.41$ is von Karman's constant and z_0 is the roughness length, which is related to the drag coefficient in eqn [2] by

$$C_{1\mathrm{m}} = \left(\frac{\kappa}{\ln(1\,\mathrm{m}) - \ln(z_0)} \right)^2 \quad [5]$$

and will be discussed later.

Equation [4] is called 'law of the wall,' and by assuming a local steady-state equilibrium between production and dissipation of turbulent kinetic energy (TKE), it can be used to estimate the vertical distribution of the turbulence dissipation rate ε

$$\varepsilon = \frac{u_*^3}{\kappa z} \quad [6]$$

Thus, in analogy to the wind-forced surface layer, the level of turbulence increases with decreasing distance from the boundary. This increasing turbulence leads, again in analogy to the surface mixed layer, to the development of a well-mixed boundary layer of up to several meters in height.

The Viscous Sublayer

It should be noted that eqn [4] is strictly valid for turbulent flows only for which the vertical transport is governed by cascading turbulent eddies. The maximum (vertical) size of the turbulent eddies is determined by the distance from the sediment surface, and by approaching the sediment surface down to scales where overturning turbulent motions are suppressed by the effect of molecular viscosity, the momentum transport becomes governed by viscous forces (first term on the right-hand side of eqn [1]). Within this layer, which is called the viscous sublayer, current shear becomes constant and the resulting linear velocity profile can be described by

$$u(z) = \frac{u_*^2}{\nu} z \quad [7]$$

On a smooth sediment surface, the viscous sublayer extends to a height δ_ν of about $10\nu/u_*$, which is comparable to the Kolmogorov microscale describing the size of the smallest turbulent eddies (typically O (1 cm), cf. **Figure 2**).

Since viscosity is reduced to its molecular value, current shear within the viscous sublayer is greater than that in the turbulent layer above (cf. **Figure 3**), a fact which has major consequences for organisms living within the viscous sublayer on the sediment surface because they have to withstand these strong shearing and overturning forces. It is further interesting to note that an appreciable amount of energy entering the BBL is dissipated within this layer (about 40%).

Effects of Bottom Roughness

The roughness length z_0 in eqn [3] determines the effective height above the bottom z at which the current velocity approaches zero. It is determined by the topographic structure of the sediment surface and

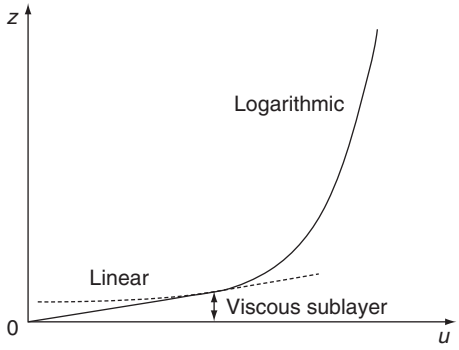

Figure 3 Velocity distribution above a smooth and rigid bottom (solid line). Within the viscous sublayer the velocity u increases linearly with distance from the sediment surface z. Above the viscous sublayer the velocity distribution follows the law of the wall (eqn [4]) and increases logarithmically with distance from the surface. Extrapolated continuations of the linear and logarithmic velocity distributions are shown as dashed lines.

hence by the typical height, width, and spacing of individual roughness elements on a stationary bed. When the scale of these roughness elements z_S is on the order of the height of the viscous sublayer δ_v or less, z_0 is solely determined by δ_v and $z_0 \approx 0.1\nu/u_*$. This flow regime is called *smooth*. When the size of the roughness elements exceeds δ_v, the flow regime is called *rough* and the corresponding roughness length is given by $z_0 \approx z_S/30$. Note that the drag coefficient $C_D \approx 1.5 \times 10^{-3}$ provided earlier (eqn [2]) corresponds to a roughness length $z_0 \approx 2.5 \times 10^{-5}$ m (eqn [5]) and hence is valid for smooth flows unless u_* exceeds 0.4 m s^{-1} or $U_{1\,m}$ exceeds 10 m s^{-1}.

In addition to the shear stress derived from viscous forces as described above (the so-called *skin friction*), larger-scale roughness elements can cause a *form drag*, which results from pressure gradients between the upstream and downstream side of particular roughness elements. Although skin friction is important for the lower part of the turbulent BBL and for the viscous sublayer, form drag resulting from, e.g., ripples, sand waves, or submerged vegetation is more important for the upper part of the turbulent BBL and for the total drag on flow. When form drag is significant, the turbulent BBL may consist of more than one logarithmic layer, described by different roughness lengths z_0, respectively.

Oscillatory Boundary Layers

The turbulent BBL equations derived here are based on steady-state conditions, i.e., on a local balance between production and dissipation of TKE, which is in equilibrium with the applied forcing. As described later, however, many forcing mechanisms for near-bottom flows are related to surface or internal waves and are hence associated with oscillatory flows. Well above the viscous sublayer, such oscillatory BBL show, similar to the effect of form drag, deviations of the of the velocity distribution from its steady-state logarithmic pattern. One major characteristic of oscillatory BBL is a pronounced maximum of the current speed at some decimeters or meters above the bed. The analytical solution to this problem (Rayleigh flow or Stokes' second problem) is an exponentially damped vertical oscillation of the current profile with a vertical wave number of $\sqrt{\omega/2\nu}$, where ω is the forcing frequency and ν the turbulent viscosity, which, however, is a function of time and distance from the sediment surface. Depending on the overall energetics of the BBL flow, characteristic current speed maxima at 2–3 m above the bed could be observed in lakes where the internal wave forcing had a period as long as 24 h. Another major consequence of oscillatory BBL is that the maximum in turbulent intensity near the bed does not coincide with the maximum of the current speed, at the top of the BBL.

Stratified BBL

Effects of Density Stratification

Density stratification affects turbulent mixing in the outer layer by causing buoyancy forces that damp or even suppress overturning turbulent eddies. The vertical distribution of velocity and turbulence described earlier for unstratified BBL may hence change significantly under stratified conditions. In addition, the vertical structure of density stratification along with the presence of sloping boundaries can introduce additional mixing phenomena in BBL of enclosed basins.

Similar to the surface mixed layer, increased production of TKE along the boundaries of a water body often leads to the generation and maintenance of a well-mixed BBL of height h_{mix}. On a flat bottom (away from the slopes) and where a logarithmic boundary layer occurs, h_{mix} can be estimated by applying scaling laws from the wind-mixed surface layer

$$h_{mix} = 2^{3/4} \frac{u_*}{\sqrt{Nf}} \qquad [8]$$

where u_* is the friction velocity in the BBL (eqn [2]), N is the Brunt–Väisälä frequency, and f is the Coriolis parameter. In small- to medium-sized water bodies, where the effect of Earth's rotation is unimportant, f has to be replaced by the respective forcing frequency, e.g., the frequency of internal seiching.

In productive water bodies, in particular, the sediment can be a significant source of remineralized nutrients as a result of microbial degradation of organic

matter at the sediment surface or within the sediment. The diffusion of solutes across the sediment–water interface (see Solute Transport and Sediment–Water Exchange section) has the potential to set up density stratification within the BBL, which could suppress turbulent mixing. Hence, whether or not a turbulent and mixed BBL can be developed and maintained depends not only on the amount of available TKE, which is typically extracted from basin-scale motions, but also on the buoyancy flux from the sediment that has to be overcome by turbulent mixing. Geothermal heating, in contrast, can result in unstable stratification and convective mixing in the BBL. A mean geothermal heat flux of 46 mW m^{-2} results in a mean vertical temperature gradient of about -8×10^{-2} K m^{-1}, which can be observed when the BBL is chemically stratified and turbulent mixing is suppressed.

2-Dimensional Mixing Processes in Enclosed Basins

The occurrence of mixed BBL (in terms of density) is a straight consequence of the application of a zero-flux boundary condition at the sediment surface, i.e., no exchange of heat and dissolved solids across the sediment–water interface. This boundary condition forces the isopycnals (or isotherms if density changes are mainly caused by temperature) to intersect the boundary at a right angle, leading to a mixed density or temperature profile in the vicinity of the boundary. Enhanced mixing along the boundaries is thus not a necessary requirement for the development of such mixed layers. Along the sloping boundaries of enclosed basins, these mixed BBL cause horizontal density gradients and hence drive horizontal currents – a process which is believed to have important consequences for basin-wide diapycnal transport.

Measurements, however, have revealed that h_{mix} is not constant along the sloping boundaries, as demonstrated in Figure 4. There the upper limit of the mixed BBL can be defined by the depth of the 5 °C isotherm (chemical stratification can be neglected in this particular lake), leading to $h_{mix} \simeq 2.3$ m in the central part of the lake, whereas $h_{mix} \leq 1$ m further up on the slopes (Figure 4(b)). The pronounced tilt of the isotherms in Figure 4(a) further emphasizes the importance of basin-scale internal waves for local estimates of h_{mix} on the slopes because the associated currents push the well-mixed BBL from the central part of the lake up and down the respective slopes during the course of the seiching.

The flow within the BBL remains parallel to the sediment surface on the sloping boundaries because the vertical velocity component must vanish at a rigid surface. Hence the flow is no longer in parallel to the isopycnals (or isotherms in Figure 4(a)) and, in combination with the fact that the flow velocity is increasing with increasing distance from the sediment surface (eqn [4]), convective instabilities can occur on the slopes when heavier water is moved on top of lighter water. Unstable stratification, as shown in the inset of Figure 4(b), can only be generated when the current is directed up-slope, a down-slope current leads to a stabilization of the BBL by the same principle. Thus, in a periodic, internal wave-driven flow, stratified and convectively mixing BBL occur alternately on the two opposing slopes of the water

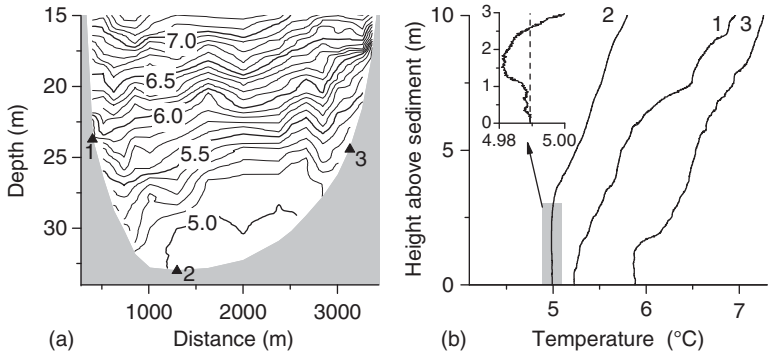

Figure 4 (a) Isotherm depths along the main axis of Lake Alpnach (Switzerland) calculated from repeated CTD profiling. The increment between neighboring isotherms is 0.1 °C and the numbers refer to the respective temperature (in °C) of the isotherms plotted as thick lines. Note that the figure is not to scale and only the lower portion of the water column is shown. The numbered symbols show the position of temperature profiles shown in (b). (b) Near-bottom temperature profiles at selected positions along the transect shown in (a). Numbers at the top of the profiles refer to the positions indicated by symbols in (a). The inset emphasizes the inverse temperature stratification observed in the BBL of profile 2. Panel (a) is adopted from Lorke A, Wüest A, and Peeters F (2005) Shear-induced convective mixing in bottom boundary layers on slopes. *Limnology and Oceanography* 50: 1612–1619, with permission from American Society of Limnology and Oceanography.

body. This shear-induced convection provides an additional source for mixing in BBL on slopes. Its general importance for BBL turbulence, however, is not yet fully understood.

Turbulence Induced by Internal Wave Interactions with Bottom Boundaries

Turbulence production in stratified regions of lakes is linked with instabilities in the internal wave field. A considerable portion of the turbulence occurs within or near the BBL and can be due to internal wave breaking at critical frequencies or internal wave steepening. Recent studies have shown that the form and degree of nonlinearity of internal waves in the thermocline can be predicted from the Wedderburn and Lake numbers, two dimensionless indices which indicate the balance between buoyancy forces and shear forces and which further take into account basin morphometry. As illustrated in Figure 5, the hypolimnion is also an internal wave field with similar wave forms to those observed in the thermocline. When Lake numbers, L_N, drop below 3, turbulence associated with the internal wave field increases (Figure 5). Thus, not only is turbulence induced in the thermocline when nonlinear waves form, but also in the hypolimnion with the greatest increases in the BBL. Values of the coefficient of eddy diffusivity increase 1–3 orders of magnitude above molecular. In small lakes, flow speeds in the BBL increase from a few millimeters per second to $\sim 2\,\mathrm{cm\,s^{-1}}$ with the decreases in Lake number.

Solute Transport and Sediment–Water Exchange

The Diffusive Sublayer

In the immediate vicinity of the sediment surface, the vertical transports of momentum and solutes (dissolved gases, solids, and heat) are reduced to their respective molecular levels, as described above. In analogy to the viscous sublayer, where momentum transport is governed by molecular viscosity, a diffusive sublayer exists, where the vertical transport of heat and solutes is governed by molecular diffusion. Since the molecular diffusivity of solutes D is about 3 orders of magnitude smaller than the molecular viscosity ν (the Schmidt number Sc, defined as $Sc = \nu/D$, is about 1000), the height of the diffusive sublayer δ_D is with $\delta_D = O(1\,\mathrm{mm})$ considerably smaller than the height of the viscous sublayer δ_ν (Figure 2). A typical profile of dissolved oxygen concentrations measured through the sediment–water interface is shown in

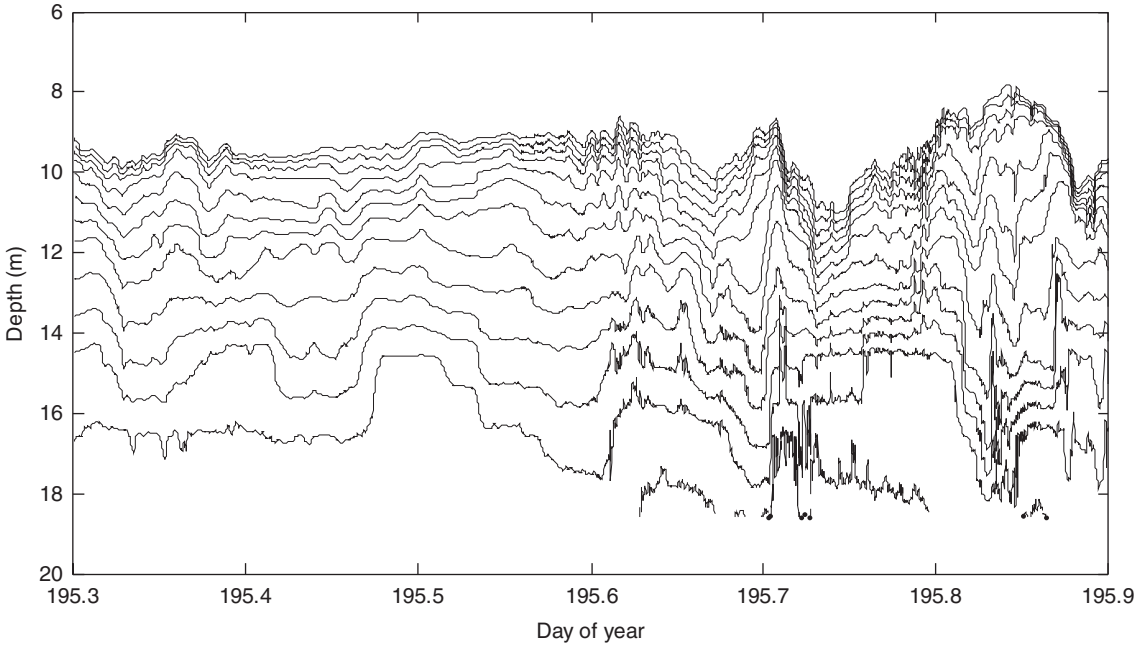

Figure 5 Isotherms illustrating the internal wave field in the hypolimnion of Toolik Lake, Alaska, prior to and after wind forcing increased to $9\,\mathrm{m\,s^{-1}}$ (day 195.6) and the Lake number decreased to 1.5. Isotherms are at 0.1 °C intervals with uppermost isotherm 6 °C. Thermistors were 80 cm apart between 10.2 and 12.6 m depth and 2 m apart deeper in the water column. Deepest thermistor was within 50 cm of the lake bottom. Increased temperature fluctuations after L_N decreases below 1.5 are indicative of turbulence either beginning or increasing in the lower water column (unpublished data, S. MacIntyre).

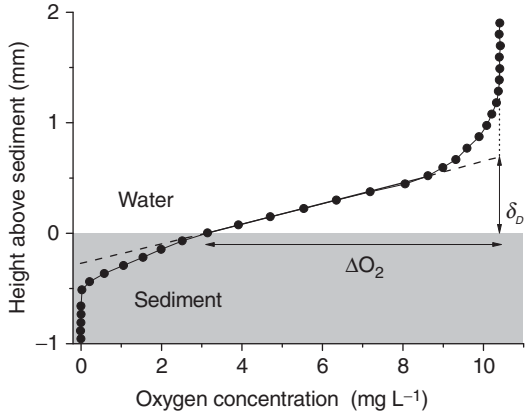

Figure 6 Oxygen concentration profile across the sediment–water interface measured in Lake Alpnach (Switzerland). The diffusive sublayer is characterized by the linear concentration gradient above the sediment surface where transport is governed by molecular diffusion. The effective height of the diffusive sublayer δ_D is defined by the intersection of the extrapolated linear concentration gradient (dashed line) with the constant oxygen concentration above the diffusive sublayer.

Figure 6. Although turbulent transport is already suppressed within the viscous sublayer, straining of concentration gradients by viscous shear results in an efficient vertical transport of solutes and to typically well-mixed solute distributions within most of the viscous sublayer. Concentration gradients are hence compressed to the diffusive sublayer overlaying the sediment surface and the constancy of the molecular diffusivity results in a linear concentration gradient $C(z)$ (Figure 6). At the top of the diffusive boundary layer, the concentration gradient decreases gradually to zero and the solute concentration reaches its constant bulk value C_∞.

Within the sediment, molecular diffusivity is reduced by the porosity (reduction of surface area) and by turtosity (increase of diffusion path length), and the concentration profile is additionally determined by chemical and microbial production and loss processes. In the case of oxygen (Figure 6), a reaction–diffusion model with rather simple zero-order kinetics of oxygen consumption resulting in a parabolic oxygen profile provides surprisingly good agreement with measured oxygen distributions.

The fluxes F of solutes through the diffusive boundary layer can be derived from Fick's first law:

$$F = \frac{D}{\delta_D}(C_\infty - C_0) \qquad [9]$$

where C_0 is the solute concentration at the sediment surface. Hence, for a given concentration gradient $(C_\infty - C_0)$ and by ignoring the temperature dependence of the molecular diffusivity, the magnitude of the flux is determined by the thickness of the diffusive sublayer δ_D. It has been demonstrated in numerous laboratory and field measurements that δ_D depends strongly on the flow regime in the turbulent BBL above. With increasing levels of turbulence (e.g., with increasing u_*) the diffusive boundary layer becomes more compressed, and according to eqn [9], the fluxes increase. The thickness of the diffusive sublayer can be related empirically to u_* or to the thickness if the viscous sublayer, which in turn is related to u_*, as described earlier:

$$\delta_D = \delta_\nu Sc^a \qquad [10]$$

where the Schmidt number Sc accounts for the different kind of 'solutes' (e.g., heat or dissolved oxygen) and observed Schmidt number exponents a range between 0.33 and 0.5. As u_* is not always an appropriate parameter for describing BBL turbulence (e.g., in oscillatory BBL or in the presence of form drag or density stratification), δ_D can also be described in terms of the Batchelor length scale, which describes the size of the smallest fluctuations of a scalar tracer in turbulent flows as a function of the turbulence dissipation rate.

It is most interesting to note that the sediment–water exchange in productive water bodies is often flux-limited by the 'bottleneck' of the diffusive sublayer and that it is actually the wind acting at the water surface that provides energy for turbulence within the BBL and hence effects the magnitude of the sediment–water fluxes by controlling the thickness of the diffusive sublayer.

Effects of Small-Scale Sediment Topography

Increased roughness of the sediment surface (e.g., due to biological activity) affects the sediment–water exchange by increasing the mass and momentum transfer as well as by increasing the surface area of the sediment–water interface. Detailed observations have demonstrated that the diffusive sublayer tends to smooth out topographic structures that are smaller than the average height of the sublayer, but smoothly follows larger roughness elements (Figure 7). The detailed structure of the oxygen distribution within the diffusive sublayer is then not only determined by diffusion (normal to the local sediment surface) but also by advection with the flow (in parallel to the local sediment surface) and it can be expected that the degree of smoothing increases with decreasing flow velocities. Detailed comparisons of measured 3-dimensional fluxes over rough topography with the fluxes calculated from the respective average diffusive sublayer heights and concentration gradients are enhanced by factors up to 49%. It must be noted, however, that fluxes estimated from concentration profiles measured at one particular location on a

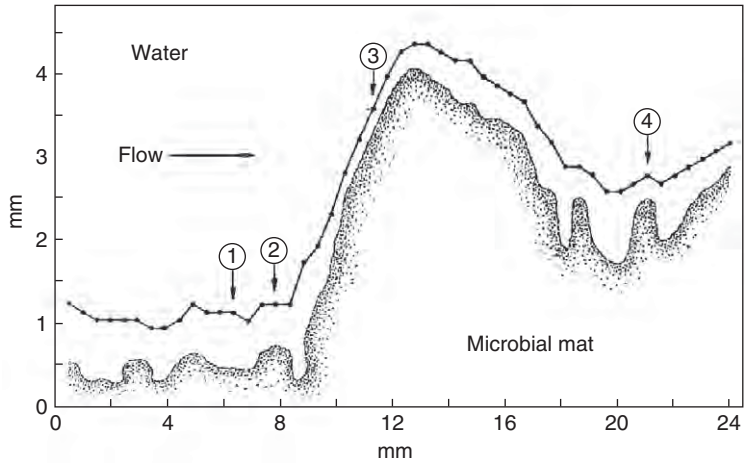

Figure 7 Horizontal transect along the direction of flow showing how the upper limit of the diffusive sublayer (solid line with data points) follows the surface topography of a microbial mat. The diffusive sublayer limit was defined by the isopleth of 90% air saturation of oxygen. Notice different vertical and horizontal scales. Flow velocity at a height of 1 cm was 4 cm s^{-1}. Numbers indicate specific measuring positions discussed in the original publication. Reproduced from Jørgensen BB and Des Marais DJ (1990) The diffusive boundary layer of sediments: Oxygen microgradients over a microbial mat. *Limnology and Oceanography* 35:1343–1355, with permission from American Society of Limnology and Oceanography.

rough sediment surface can severely overestimate or underestimate the average flux, as demonstrated in Figure 7.

Nondiffusive Fluxes

Besides the diffusive fluxes, there exist several additional pathways for the exchange of solutes across the sediment–water interface. Convectively driven transport of pore water through the interface can occur in shallow waters where shortwave solar radiation penetrates the water column to the sediment surface and heats the sediment. Similarly, changes in temperature of the water overlaying the sediment surface, e.g., due to internal waves in stratified water bodies, have been observed to drive convective transport across the sediment–water interface. The existence of larger roughness elements, such as ripples, on permeable sediments can further result in advective pore water exchange driven by pressure differences. Higher dynamic pressure at the upstream side of such topographic structures give rise to the transport of water into the sediment, whereas the lower pressure at the downstream side sucks pore water out of the sediment.

Bioturbation and *bioirrigation* are processes by which benthic fauna or flora enhances the sediment–water exchange. Whereas bioturbation mainly refers to the displacement and mixing of sediment particles by, e.g., worms, bivalves, or fish, bioirrigation refers to the flushing and active ventilation of burrows with water from above the sediment surface. These processes are particularly important in oligotrophic water bodies where the sediment surface remains oxic and provides suitable conditions for a diverse benthic fauna. In more eutrophic systems the emanation of gas bubbles (mainly methane or carbon dioxide) which are formed by biogenic production and a resulting supersaturation of pore water with these gases may have similar effects.

In Situ Flux Measurements

The sediment oxygen demand or the release of nutrients from the sediment can be of major importance for the overall productivity and for the geochemical composition of a particular water body and quantification of sediment–water fluxes is often essential for understanding biogeochemical cycles within the water column. As these fluxes depend strongly on the hydrodynamic conditions in the BBL and as these conditions have a strong spatial and temporal dynamics, in situ measurements are often desirable. The measurement of concentration profiles through the sediment–water interface capable of resolving the diffusive sublayer are one way for estimating the fluxes. From a measured profile of dissolved oxygen, as shown in Figure 6, the sediment–water flux can be readily estimated by applying eqn [9]. Such measurements are carried out using microelectrodes, which are available for a large number of solutes, mounted on a benthic lander system. However, there are two major problems associated with this method: First, although these microelectrodes have tiny tip

diameters (down to 10 μm or less for oxygen sensors), they were demonstrated to disturb the concentration distribution within the diffusive boundary layer while profiling. The second and more severe problem results from the complexity of the spatial distribution of the fluxes resulting not only from the small-scale sediment topography (cf. Figure 7) but also from the strongly localized effects of advective pore water exchange and bioturbation. To overcome these problems, the flux can be measured within the turbulent BBL at some distance from the actual sediment surface. By neglecting any sources or sinks within the water column between the sampling volume and the sediment surface, this flux represents an areal average of the sediment–water flux including all non-diffusive flux contributions. The turbulent flux F_{turb} is determined by the cross-correlation of turbulent vertical velocity (w') and turbulent concentration (C') fluctuations:

$$F_{\text{turb}} = \overline{w'C'} \qquad [11]$$

where the overbar denotes temporal averaging.

Particle Dynamics

BBLs are often characterized by enhanced concentrations of suspended particles as compared to the water column above. Such nepheloid layers are generated by resuspension of particles from the sediment surface and subsequent upward transport. The potential of a turbulent flow to entrain sediment particles of size D is often described in a Shields diagram where empirical thresholds of sediment motion are provided as a function of a nondimensional shear stress $\theta = \rho u_*^2/((\rho_p - \rho)gD)$ and a particle Reynolds number $Re_* = u_* D/\nu$, in which ρ_{p} is the particle density and g the gravitational constant. The θ can be interpreted as the ratio between the lift force provided by the turbulent shear stress defined in eqn [3] and the gravitational force acting on the particle. While in suspension, the fate of the particle is determined by the balance between upward transport by turbulent diffusion and Stokes settling.

The quantitative characterization of resuspension and particle transport, however, is often complicated by cohesive properties of the particles. Cohesive particles require greater shear stresses to become resuspended; moreover, they tend to form aggregates when in suspension, which alters their settling velocities.

The resuspension–settling cycles increase the contact area between particle surfaces and water and thus enhance the fluxes from and to the particles. In addition, suspended particles contribute to water density and locally enhanced resuspension, generated, e.g., by high near-bottom current velocities in the littoral zone or at the depth of the thermocline (cf. Figure 1), may lead to the formation of turbidity currents.

Glossary

Dissipation rate of TKE – Rate of dissipation of TKE per unit volume of water and per unit time. This energy is dissipated into heat by internal friction among fluid elements described by viscosity.

Nepheloid layer – Particle-rich layer above the sediment. This layer is sustained by a balance between gravitational settling and turbulent vertical diffusion counteracting it.

Pore water – Water that fills the interstitial space between sediment grains.

Reynolds number – The dimensionless Reynolds number Re is the ratio of inertial to viscous forces acting on a fluid element, obstacle in the flow, or submerged organism and describes the transition from laminar to turbulent flow regimes.

Shear stress – Force per unit area acting in parallel (tangential) to the surface of a fluid element or interface (e.g., bed shear stress).

Turbulent eddies – Turbulence is composed of eddies: patches of zigzagging, often swirling fluid, moving randomly around and about the overall direction of motion. Technically, the chaotic state of fluid motion arises when the speed of the fluid exceeds a specific threshold, below which viscous forces damp out the chaotic behaviour (see also *Reynolds number*).

Turbulent kinetic energy – Kinetic energy per unit volume of water, which is contained in the random fluctuations of turbulent motions. Turbulent velocity fluctuations u' can be separated from the mean current velocity $\bar{u}$ by Reynolds decomposition of the actual velocity u ($u = \bar{u} + \text{u}'$). Turbulent kinetic energy (TKE) is then defined by, $TKE = 1/2\rho u'^2$, where ρ denotes density of water.

See also: Biological-Physical Interactions; Currents in Rivers; Currents in Stratified Water Bodies 1: Density-Driven Flows; Currents in Stratified Water Bodies 2: Internal Waves; Currents in Stratified Water Bodies 3: Effects of Rotation; Currents in the Upper Mixed Layer and in Unstratified Water Bodies; Density Stratification and Stability; Flow Modification by Submerged Vegetation; Small-scale Turbulence and Mixing: Energy Fluxes in Stratified Lakes; The Surface Mixed Layer in Lakes and Reservoirs.

Further Reading

Ackerman JD, Loewen MR, and Hamblin PF (2001) Benthic–Pelagic coupling over a zebra mussel reef in western Lake Erie. *Limnology and Oceanography* 46: 892–904.

Berg P, *et al.* (2003) Oxygen uptake by aquatic sediments measured with a novel non-invasive eddy-correlation technique. *Marine Ecology Progress Series* 261: 75–83.

Boudreau BP and Jørgensen BB (2001) *The Benthic Boundary Layer.* New York: Oxford University Press.

Caldwell DR and Chriss TM (1979) The viscous sublayer at the sea floor. *Science* 205: 1131–1132.

Gloor M, Wüest A, and Münnich M (1994) Benthic boundary mixing and resuspension induced by internal seiches. *Hydrobiology* 284: 59–68.

Gundersen JK and Jørgensen BB (1990) Microstructure of diffusive boundary layers and the oxygen uptake of the sea floor. *Nature* 345: 604–607.

Lorke A, Müller B, Maerki M, and Wüest A (2003) Breathing sediments: The control of diffusive transport across the sediment-water interface by periodic boundary-layer turbulence. *Limnology and Oceanography* 48: 2077–2085.

Lorke A, Umlauf L, Jonas T, and Wüest A (2002) Dynamics of turbulence in low-speed oscillating bottom-boundary layers of stratified basins. *Environmental Fluid Mechanics* 2: 291–313.

Lorke A, Wüest A, and Peeters F (2005) Shear-induced convective mixing in bottom boundary layers on slopes. *Limnology and Oceanography* 50: 1612–1619.

Mellor GL (2002) Oscillatory bottom boundary layers. *Journal of Physical Oceanography* 32: 3075–3088.

Miller MC, Mccave IN, and Komar PD (1977) Threshold of sediment motion under unidirectional currents. *Sedimentology* 24: 507–527.

Wüest A and Gloor M (1998) Bottom boundary mixing: The role of near-sediment density stratification. In: Imberger J (ed.) *Physical Processes in Lakes and Oceans. Coastal and Estuarine Studies*, pp. 485–502. American Geophysical Union.